Part Load Resonance Risk Assessment of Francis Hydropower Units

J. Gomes P. Jr.[(1)], *A. Favrel*[(1)], *C. Nicolet*[(2)], *F. Avellan*[(1)]

[(1)]Laboratory for Hydraulic Machines, EPFL, Lausanne, Switzerland
[(2)]Power Vision Engineering Sàrl, Ecublens, Switzerland
corresponding author e-mail address: joao.gomes@epfl.ch

ABSTRACT

While operating at part load, Francis turbines feature a precessing cavitation vortex rope in its draft tube. The precession of this vortex in the elbow of the draft tube acts as a pressure pulsation source which frequency can match the first hydroacoustic eigenfrequency of the hydraulic system in some cases. Resonance phenomenon can be predicted by using reduced scale physical model tests and numerical simulations, but it remains challenging. This paper proposes a procedure to estimate the risk of part load resonance at the early stage of a hydropower project. The proposed procedure uses the hydroacoustic properties of a given reduced scale physical model and applies them to a large number of turbine designs and power plant configurations to assess the risk of resonance for each one of them. Results show that resonance are likely to occur in hydropower plants in a certain range of turbine rated head and rated discharge values. These results can then indicate if more detailed investigations in some specific hydropower projects are necessary.

KEYWORDS

cavitation, Francis turbine, hydroacoustic, part load, resonance, vortex rope

NOMENCLATURE

A pipe cross-section area (m^2)
a wave speed ($m \cdot s^{-1}$)
C_c cavitation compliance (m^2)
C_{eq} total equivalent compliance (m^2)
Cm amplitude of the $\vec{Cm}$ vector ($m \cdot s^{-1}$)
D runner outlet external diameter (m)
E turbine specific energy ($J \cdot kg^{-1}$)
Fr Froude number ($\cdot$)
f_0 first system eigenfrequency (Hz)
f_{vortex} vortex precession frequency (Hz)
g gravity ($m \cdot s^{-2}$)
H turbine net head (m)
h piezometric pressure (m)
L pipe length (m)
N runner rotation speed (min^{-1})
n_{ED} IEC speed factor ($\cdot$)
NPSE Net Positive Suction Specific Energy ($J \cdot kg^{-1}$)
n_{QE} IEC specific speed ($\cdot$)
Q discharge ($m^3 \cdot s^{-1}$)
Q_{ED} IEC discharge factor ($\cdot$)
S swirl number ($\cdot$)
V_c cavitation volume (m^3)

Greek letters
σ Thoma number ($\cdot$)
ω runner rotation speed (rad s^{-1})

vectors
$\vec{C}$ flow velocity
$\vec{Cm}$ meridian component of the flow velocity
$\vec{Cu}$ peripheral component of the flow velocity
$\vec{U}$ runner blade trailing edge peripheral velocity
$\vec{W}$ relative velocity

subscripts
$_0$ swirl free condition
$_{rated}$ rated value

INTRODUCTION

Francis turbines are designed to operate under a certain range of head and discharge values that may vary according to the site conditions where they are installed. Compared to other types of hydraulic turbines, such as Kaplan and Pelton, Francis turbines usually present the advantage of having the highest peak efficiency values.

However, on the downside, Francis turbines feature fixed blades, preventing them to better adapt to head and discharge variations. As a result, at off-design conditions, part of the angular momentum present in the flow is not recovered by the runner and a swirling flow is observed at the runner outlet. It gives rise to the development in the draft tube of the so-called vortex rope that features a low-pressure core and can cavitate in case the downstream reservoir water level is not high enough to keep the pressure in the vortex core above the vapor pressure.

In part load conditions, the vortex rope will also induce a synchronous pressure pulsation that has the same frequency as the precession frequency of the vortex, usually between 20% and 40% of the runner rotation frequency [1, 2, 3]. In the case where cavitation appears in the vortex core, a higher cavitation compliance causes a drop of the hydraulic circuit eigenfrequency values. Resonance occurs if one of the eigenfrequencies matches the pressure pulsation frequency generated by the vortex, as observed in the test case presented by Arthur *et al.*[4]. A detailed study is performed by Nicolet *et al.*[5] to assess the risk of resonance in part load condition of a given hydropower plant featuring four generating units sharing the same penstock.

The amplitude of the pressure pulsations is amplified in case of resonance, which may cause power swings and harm the hydro-mechanical components [6]. Fortunately, this phenomenon

is known to happen in the operating range of only a small number of generating units as it depends on a combination of a large number of different parameters, such as the length and compliance of the pipes in the hydraulic circuit, the runner rotation speed, the runner diameter and the downstream reservoir water level. An outlook on this type of resonance phenomena is provided by Nishi& Liu in [7].

This paper proposes a procedure to estimate what are the hydropower projects that have a higher risk of presenting part load resonance phenomenon. For this purpose, the hydroacoustic properties of the cavitating vortex rope obtained from measurements in a given turbine test case is taken as a reference. These reference values are assumed to be representative to any Francis turbine design and are then transposed and applied to a large number of power plant configurations where typical values of turbine runner diameter and rotation speed are derived [8]. Two possibilities for the penstock are assumed: a long penstock with low wave speed and a short penstock with high wave speed, as the hydroacoustic properties of most power plants fall in between these two cases. Finally, a 1-D numerical model of each hypothetical power plant project is used to calculate its first eigenfrequency value while operating at different discharge values inside the part load condition. In case this first eigenfrequency can match the vortex excitation frequency, the hypothetical power plant project is identified as having a higher risk of resonance.

The final aim of this paper is to help design engineers working in the early stage of a given hydropower plant project to assess if a part load resonance phenomenon is likely to occur. A given range of turbine rated head and rated discharge values is identified as having higher risk of presenting part load resonance. It can then help justifying the investment in further investigations once detailed information on the hydraulic circuit and turbine are available. Detecting and mitigating the risk of resonance in the early design stage may reduce future operational costs, as it can avoid a reduction in the turbine operating range or necessity of air injection.

PART LOAD VORTEX ROPE AND CAVITATION COMPLIANCE

Francis turbine prototypes recover hydraulic power and transfer it to an electric generator through a shaft. As generators for hydropower units are usually of synchronous type, while they are connected to the power grid they keep the rotation speed of the turbine at a practically constant value. In this case, for a given head value H inside the operating range of the turbine, there is a unique discharge value Q_0 where the tangential component of the flow velocity vector, $\vec{Cu}$, have zero magnitude at the runner outlet. In part load conditions, when the discharge is lower than Q_0, the magnitude of $\vec{Cu}$ is greater than zero and the flow rotates with the same direction as the runner. This condition is illustrated by the velocity diagram in Figure 1a, where the part load condition is indicated in red. If the ratio between axial and tangential flow momentum is high enough, a precessing vortex develops in the draft tube at the runner outlet. If pressure levels are sufficiently low, cavitation can be observed in the vortex rope core, as illustrated in Figure 1b. The dynamic characteristics of the vortex rope is closely related to the flow swirl number S, defined as the ratio between the axial flux of angular momentum and the axial flux of axial momentum [9]. By considering the velocity diagram at the runner outlet as the one in Figure 1a, A. Favrel *et al.*[3] derived the following equation to estimate S at the runner outlet of a Francis turbine:

$$S = \frac{\omega D}{4}\left(\frac{1}{Cm} - \frac{1}{Cm_0}\right) = n_{\mathrm{ED}}\frac{\pi^2}{8}\left(\frac{1}{Q_{\mathrm{ED}}} - \frac{1}{Q_{\mathrm{ED}_0}}\right) \tag{1}$$

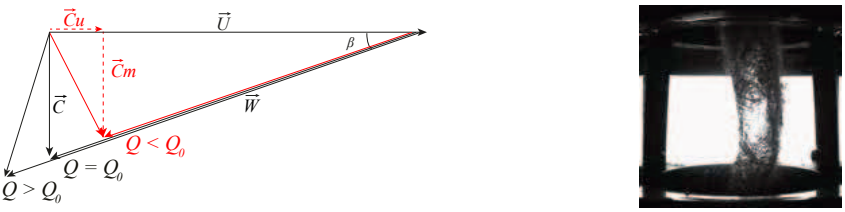

(a) (b)

Figure 1: (a) **Flow velocity diagram at the runner trailing edge. The part load condition where $Q < Q_0$ is indicated in red.** (b) **Visualization of a part load cavitation vortex rope in the draft tube cone of a reduced scale physical turbine model.**

where n_{ED} and Q_{ED} are the IEC non-dimensional speed and discharge factors, defined as in Equation 2.

$$n_{\text{ED}} = \frac{ND}{60\sqrt{E}} \qquad Q_{\text{ED}} = \frac{Q}{D^2\sqrt{E}} \qquad E = gH \tag{2}$$

The intensity of the vortex is mainly given by the swirl number S. Meanwhile, two other numbers have an impact in the local pressure and determine the presence of cavitation and its volume: the Thoma number σ and the Froude number Fr (see [10]), defined as $\sigma = \text{NPSE}/E$ and $\text{Fr} = \sqrt{E/gD}$. Once cavitation inception occurs in the vortex core, the total compliance of the flow increases drastically, causing a sudden drop of the pressure wave speed in the draft tube cone, lowering the eigenfrequencies of the whole hydraulic system [11]. The cavitation compliance C_{c}, first defined in [12], and its relation with the pressure wave speed a are presented in Equation 3, as detailed in [11, 13].

$$a = \sqrt{\frac{gAL}{C_{\text{eq}}}} \qquad C_{\text{eq}} = C_{\text{water}} + C_{\text{pipe}} + C_{\text{c}} \qquad C_{\text{c}} = -\frac{\partial V_{\text{c}}}{\partial h} \quad (\text{m}^2) \tag{3}$$

As the cavitation compliance is generally much greater than the sum of the liquid water compliance C_{water} and the compliance due to the pipe deformation C_{pipe}, it can be assumed $C_{\text{eq}} \approx C_{\text{c}}$ in cavitating conditions. In non-cavitating conditions, C_{pipe} and C_{water} determine the pressure wave speed. Typical values of pressure wave speeds in steel-lined penstocks are between 1000 $\text{m}\cdot\text{s}^{-1}$ and 1300 $\text{m}\cdot\text{s}^{-1}$ (see [14]), but lower values such as 400 $\text{m}\cdot\text{s}^{-1}$ are possible especially in penstocks made of polymeric material (see [15]). More detailed equations for the calculation of pressure wave speed values in non-cavitating conditions are provided in [16, 17].

REFERENCE VALUES OF CAVITATION COMPLIANCE

The C_{c} value in the draft tube cone of a reduced scale physical model of a Francis turbine operating at part load is determined by combining reduced scale model measurements and 1-D eigenvalue calculations of the test rig, as discussed in [18]. An excitation system is attached to the test rig and is used to make apparent the first eigenfrequency of the whole hydraulic system. As the hydroacoustic properties of all the other parts of the test rig are known and remain constant, the C_{c} value in the draft tube cone is obtained by matching measured and calculated test rig first eigenfrequency values. The eigenfrequency calculations are performed using a 1-D numerical model constructed using the SIMSEN software. Detailed information on the mathematical model of hydraulic components such as the Francis turbine and the pressurized

Table 1: Fr, σ and S values in which measurements are performed on the reference reduced scale physical model.

Fr $(\cdot)$	$\sigma\,(\cdot)$	$S\,(\cdot)$
5.52	0.110	[0.63 , 1.77]
6.57	0.110	1.31
7.65	0.110	1.30
8.74	0.096	[0.63 , 1.76]
8.74	0.110	[0.63 , 1.77]
8.74	0.128	[0.98 , 1.50]

pipes contained in the SIMSEN software is found in [16]. Detailed information on the cavitating draft tube mathematical model is found in [13, 11].

The methodology mentioned above to identify C_c values is applied to a reduced scale physical model of a Francis turbine with IEC specific speed $n_{QE} = 0.131$, featuring a runner with $D_{model} = 0.35$ m of external diameter. Detailed information on the test rig, the excitation system and the 1-D SIMSEN model used in the procedure are found in [11]. The Fr, σ and S values in which measurements are performed to determine C_c values are listed in Table 1. The resulting values of C_c obtained in this measurements campaign are shown in Figure 2. The presented C_c values correspond to the total cavitation compliance in the one meter long draft tube cone of the reference reduced scale physical turbine model. The turbine draft tube cone is simulated using 32 elements, each with a local cavitation compliance of $C_c/32$. The remaining part of the draft tube, the diffuser, is simulated using 3 elements with 400 m·s^{-1} wave speed in its first 1.1 m, followed by 6 elements with 200 m·s^{-1} wave speed in its remaining 2.5 m. These wave speed values are based on the results presented by [2].

Using a non-linear least-squares method, a best fit interpolation function $\hat{f}_C\,(\sigma, S, \mathrm{Fr})$ is derived from the performed measurements to estimate C_c at any operating condition in part load. The resulting $\hat{f}_C$ function shown in Figure 2 approximates the measured C_c values with a resulting standard deviation of 0.46×10^{-3} m^2.

By using dimensional analysis and considering two homologous Francis turbines operating

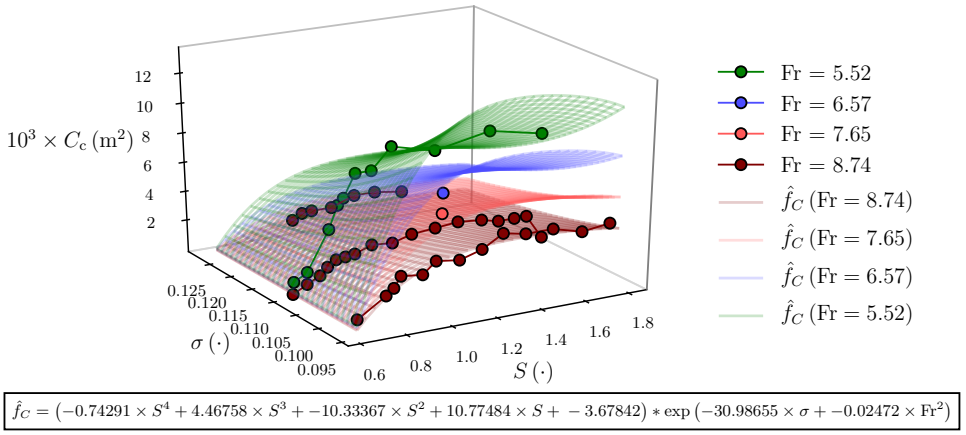

Figure 2: **Resulting values of C_c obtained through a measurements campaign as a function of σ, S and Fr values. The resulting interpolation function $\hat{f}_C$ is also presented.**

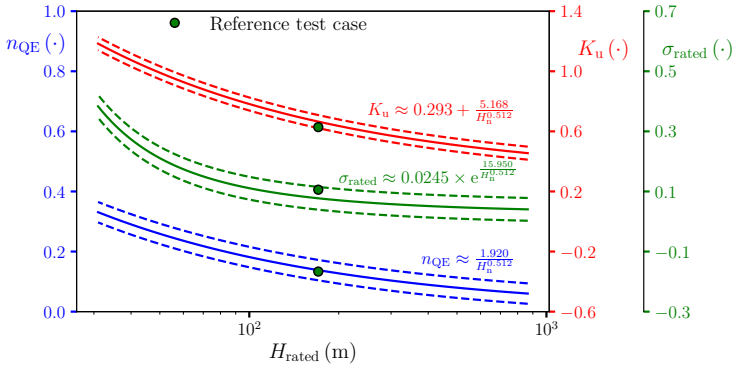

Figure 3: **Relations between H_{rated}, N_q, σ_{rated} and K_u obtained by [8]**

at the same conditions of Fr, S and σ, the transposition of C_c values from model to prototype scale can be performed as in Equation 4.

$$C_{c_{proto}} = C_{c_{model}} \times \left(\frac{D_{proto}}{D_{model}}\right)^2 \approx f_C(\sigma, S, Fr) \times \left(\frac{D_{proto}}{D_{model}}\right)^2 \tag{4}$$

where $f_C(\sigma, S, Fr) = \max\left[\hat{f}_C(\sigma, S, Fr), 0\right]$ in order to have $C_{c_{proto}} = 0$ in cases where $0 < S < 0.63$, the part load S values in which no cavitation is observed.

RISK OF RESONANCE ASSESSMENT PROCEDURE

Once the turbine rated head value is known, Francis turbines manufactures tend to design turbines with very similar n_{QE} value. As a consequence, other design variables such as σ_{rated} and K_u, defined as in Equation 5, can also be estimated empirically. Using a large database of Francis turbines, the relations between H_{rated}, N_q, σ_{rated} and K_u obtained by Lugaresi and Massa [8] are presented in Figure 3.

$$K_u = \frac{\pi DN}{60\,(2gH_{rated})^{0.5}} = \frac{\pi}{\sqrt{2}} n_{ED_{rated}} \tag{5}$$

According to [8], the turbine diameter D_{proto} can be estimated by assuming 10.7 m·s^{-1} of mean axial flow velocity at the runner outlet when operating at Q_{rated}. As a result, by knowing only H_{rated} and Q_{rated} of the Francis turbine generating unit, values of σ_{rated}, Fr_{rated} and S at part load conditions can be estimated. Finally, by knowing that Francis turbine have very similar geometric and kinematic properties, it is assumed that the C_c values obtained with the reference test case are representative, allowing the use of Equation 4 to estimate $C_{c_{proto}}$ in other test cases as an approximation.

The following procedure is then applied to estimate what are the hydropower plant configurations and Francis turbine design choices that present a higher risk of resonance between the first eigenfrequency of the plant hydraulic circuit and the excitation frequency of the vortex rope:

1. From H_{rated} and Q_{rated}, use the empirical relations proposed by Lugaresi and Massa [8] to define σ_{rated} and Fr_{rated} values. The S values at part load are obtained using Q values in the $[0.5 \times Q_{rated}, 0.9 \times Q_{rated}]$ interval. Discharge values leading to S values greater than 1.77 are ignored as $S = 1.77$ is the highest measured value in the reduced scale model. This limitation only affects a small number of high H_{rated} turbines;

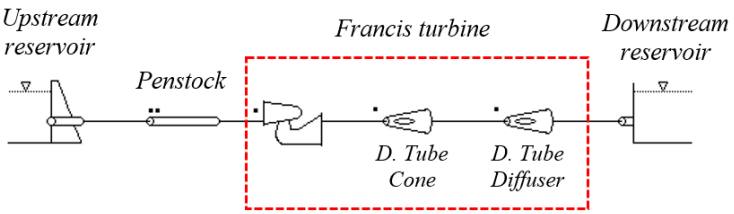

Figure 4: **Numerical simulation of the simplified hydropower plant hydraulic circuit.**

2. Calculate $C_{c_{proto}}$ using σ_{rated}, Fr_{rated}, D_{proto} and the part load S values in Equation 4. Some extrapolation of the measurements range used to generate Equation 4 is necessary, but those are usually conditions with high Fr_{rated} or high σ_{rated} values, both leading to very small C_c values, as captured by Equation 4;

3. Use the data from the previous steps in the numerical simulation of the simplified hydropower plant hydraulic circuit of Figure 4 to calculate the first eigenfrequency of the hydraulic system f_0 for each S value;

4. Assume the vortex precessing frequency as $f_{vortex} = 0.3 \times N/60$. If there is a possibility of having $f_0 = f_{vortex}$, risk of resonance is assumed for this hydropower plant project test case.

The length of the hydropower plant penstock has a direct impact on f_0, specially in non-cavitating conditions. Knowing that most of the plants feature penstock length values between $L = H_{rated}$ and $L = 2 \times H_{rated}$, these two extreme possibilities are assumed for the numerical simulations. The same reasoning is applied to the pressure wave speed: the wave speed in the short version of the penstock is fixed at $a = 1480\ \mathrm{m \cdot s^{-1}}$, equal to the wave speed in water at 20 °C, while the long version of the penstock is fixed at $a = 700\ \mathrm{m \cdot s^{-1}}$, *i.e.*, $C_{pipe} \approx 3.5 \times C_{water}$ of additional compliance is considered. Consequently, the short penstock case with high wave speed features greater values of f_0 than the long penstock case.

In case the cavitation compliance in the draft tube cone becomes $C_{c_{proto}} \approx 0$, the maximum value of wave speed inside the draft tube cone is assumed to be $a = 1000\ \mathrm{m \cdot s^{-1}}$. In the remaining parts of the draft tube where no cavitation is expected, *i.e.*, the elbow and the diffuser, the wave speed is assumed to have a constant value of $a = 1000\ \mathrm{m \cdot s^{-1}}$. The turbine itself being a small part of the whole hydraulic circuit, the assumed wave speed values in non-cavitating conditions inside the turbine parts are expected to have only a small impact in the final results.

RESULTS

The described procedure is applied to a large interval of possible H_{rated} and Q_{rated} values containing all the values in which Francis turbines are normally designed. To better illustrate the results, typical f_0 curves for the short penstock case and the long penstock case as a function of Q are shown in Figure 5a. As indicated, the results are separated in four groups according to the position of f_{vortex} with respect to the f_0 curves:

1. The estimated f_{vortex} value is higher than any calculated f_0 value, for both short and long penstock cases. No risk of resonance with the first hydraulic system eigenfrequency is possible, but higher-order eigenfrequencies may be excited. These cases are beyond the scope of this paper;

2. The f_{vortex} value crosses the f_0 curve in the short penstock case only, indicating risk of resonance in this case;

3. The f_{vortex} value crosses the f_0 curves of the short and the long penstock cases, indicating risk of resonance in both.

4. The f_{vortex} value remains below the f_0 curve, so no resonance is possible. For the blue area indicated in the graph of Figure 5b, the f_0 curve of the short penstock case is considered.

Although not indicated in Figure 5, an interval of H_{rated} and Q_{rated} values where resonance only in the long penstock case is detected is also possible. Nevertheless, this condition was not observed in the chosen test cases as it would represent a very small interval in the border between groups (3) and (4). Simulations were also performed assuming $f_{\text{vortex}} = 0.2 \times N/60$ and $f_{\text{vortex}} = 0.4 \times N/60$, resulting in some cases in a shift towards the neighboring points located just above or just below the presented results for $f_{\text{vortex}} = 0.3 \times N/60$, respectively.

The interval of H_{rated} and Q_{rated} values where part load resonance is expected is presented in Figure 5b. This interval contains the reference test case values and those for three other cases described in [19, 20, 21], where part load resonance is indeed observed in the prototype. As illustrated in Figure 5b, the interval in which the risk of resonance is predicted is larger for the short penstock case, as it combines the intervals indicated by (2) and (3), than the interval for the long penstock case, indicated by (3). The higher risk of resonance for the short penstock case is explained by the larger decrease in f_0 values from a non-cavitating to a cavitating condition.

Considering a given H_{rated} value, it is noted that turbines with lower Q_{rated} values present less risk of resonance, as their smaller diameter leads to lower $C_{\text{c}_{\text{proto}}}$ values and less variations of f_0.

CONCLUSIONS

This paper presents a procedure to point out what are the Francis turbine design and power plant configurations that present a higher risk of resonance between the hydraulic system first eigenfrequency and the vortex rope precession frequency at part load. The procedure uses values of cavitation compliance in the draft tube measured in a reduced scale physical turbine model as a reference. These values are transposed and applied to different turbines with different rated head and rated discharge values.

The results lead to the following conclusions: 1) resonance is likely to occur in hydropower projects containing turbines designed within a certain range of rated head and rated discharge values. This range corresponds to rated head values where the turbine draft tube $C_{\text{c}_{\text{proto}}}$ values in part load conditions are the *highest, allowing large variations of* f_0 ; 2) hydropower plants featuring a *short penstock* present a higher risk of resonance than those with long penstocks; 3) hydropower Francis units with the highest rated head values feature a part load vortex rope with precession frequency higher than the first hydraulic system eigenfrequency. *Resonance with eigenfrequencies of a higher order can occur* in these cases, but this aspect is beyond the scope of this paper

It must be emphasized that the presented procedure cannot predict with certainty the occurrence of resonance in a given hydropower plant. For this purpose, a detailed 1-D numerical model of the Francis unit and the whole hydraulic system is required, including the real dimensions and wave speed values of every part of the circuit. This type of study would also require measurements of the cavitation compliance in the draft tube of the reduced scale physical model

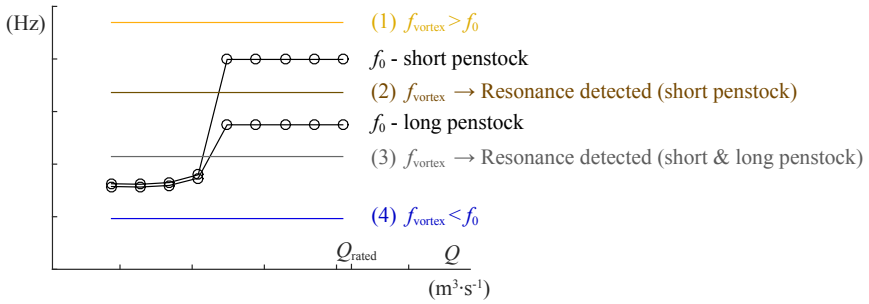

(a)

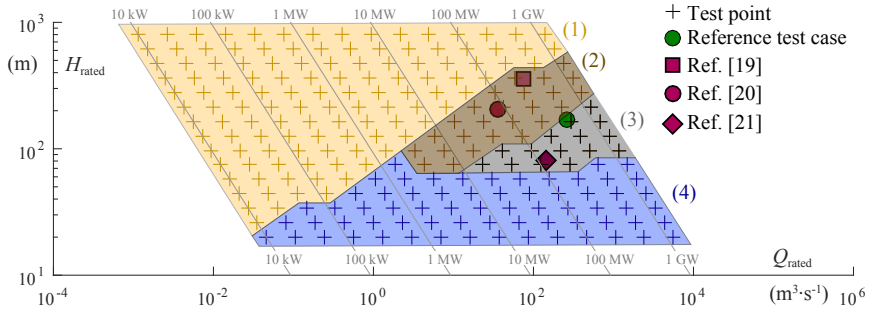

(b)

Figure 5: a) **Typical f_0 curves for the short penstock case and the long penstock case, as a function of Q in part load conditions. Results are separated in four groups according to the position of f_{vortex} with respect to the f_0.** b) **H_{rated} and Q_{rated} values where the procedure is applied. Real cases where part load resonance conditions were detected are also indicated.**

of a Francis turbine homologous to the one used in the project. Nevertheless, performing this type of measurements is expensive and time consuming, but may be justified in case a high risk of resonance is detected. That would be the case for the three generating units, studied by other authors and mentioned in the results section, which rated head and rated discharge values are within the predicted range of risk. The results presented in this paper can then be seen as a guideline, showing the cases where further investigations might be worth the investment.

ACKNOWLEDGMENTS

The authors would like to thank BC Hydro (CA) for making available the reduced scale physical model. Additionally, the research leading to the results presented in this paper is part of the HYPERBOLE research project, granted by the European Commission (ERC/FP7-ENERGY-2013-1-Grant 608532) and the RENOVHydro project, granted by the CTI, Commission for Technology and Innovation and the SFOE, Swiss Federal Office of Energy.

REFERENCES

[1] P. Dériaz. A contribution to the understanding of flow in draft tubes of francis turbines. IAHR Section Hydraulic Machinery, Equipment, and Cavitation, 1st Symposium (Nice, 1960), paper B-1, 1960.

[2] J. Arpe. *Analyse du champ de pression pariétale d'un diffuseur coudé de turbine Francis*. PhD thesis, Lausanne, 2003.

[3] A. Favrel, J. Gomes P. Jr., C. Landry, A. Müller, C. Nicolet, and F. Avellan. New insight in francis turbine cavitation vortex rope: role of the runner outlet flow swirl number. *Journal of Hydraulic Research*, 56(3):367–379, 2018.

[4] A. Favrel, J. Gomes P. Jr, C. Landry, S. Alligné, L. Andolfatto, C. Nicolet, and A. Avellan. Prediction of hydro-acoustic resonances in hydropower plants by a new approach based on the concept of swirl number. Manuscript submitted for publication, 2018.

[5] C. Nicolet, J.-J. Herou, B. Greiveldinger, P. Allenbach, J.-J. Simond, and F. Avellan. Methodology for risk assessment of part load resonance in francis turbine power plant. In *Proceedings IAHR Int. Meeting of Working Group on Cavitation and Dynamic Problems in Hydraulic Machinery and Systems*, number LMH-CONF-2007-004, 2006.

[6] R. Guarga, G. Hiriart, and J. Torres. Oscillatory problems at mexico's la angostura plant. *Water Power and Dam Construction*, 35:33–6, 1983.

[7] M. Nishi and S. Liu. An outlook on the draft-tube-surge study. *International Journal of Fluid Machinery and Systems*, 6(1):33–48, 2013.

[8] A. Lugaresi and A. Massa. Designing francis turbines: trends in the last decade. *International Water Power and Dam Construction IWPCDM*, 39(11), 1987.

[9] A. K. Gupta, a. G. Lilley, and N. Syred. Swirl flows. *Tunbridge Wells, Kent, England, Abacus Press, 1984, 488 p.*, 1984.

[10] J. Gomes, A. Favrel, C. Landry, C. Nicolet, and F. Avellan. Measurements of cavitation compliance in the draft tube cone of a reduced scale francis turbine operating at part load. In *Proceedings of the 10th International Symposium on Cavitation, CAV2018*, 2018.

[11] C. Landry. *Hydroacoustic Modeling of a Cavitation Vortex Rope for a Francis Turbine*. PhD thesis, Lausanne, 2015.

[12] C. Brennen and A. Acosta. Theoretical, quasi-static analysis of cavitation compliance in turbopumps. *Journal of Spacecraft and Rockets*, 10(3):175–180, 1973.

[13] S. Alligne, C. Nicolet, Y. Tsujimoto, and F. Avellan. Cavitation surge modelling in francis turbine draft tube. *Journal of Hydraulic Research*, 52(3):399–411, 2014.

[14] F. Hachem and A. Schleiss. A review of wave celerity in frictionless and axisymmetrical steel-lined pressure tunnels. *Journal of Fluids and Structures*, 27(2):311–328, 2011.

[15] A. Triki. Water-hammer control in pressurized-pipe flow using a branched polymeric penstock. *Journal of Pipeline Systems Engineering and Practice*, 8(4):04017024, 2017.

[16] C. Nicolet. *Hydroacoustic modelling and numerical simulation of unsteady operation of hydroelectric systems*. PhD thesis, Lausanne, 2007.

[17] V. L. Streeter and E. B. Wylie. Hydraulic transients. Technical report, mcgraw-hill, 1967.

[18] C. Landry, A. Favrel, A. Müller, C. Nicolet, and F. Avellan. Local wave speed and bulk flow viscosity in francis turbines at part load operation. *Journal of Hydraulic Research*, 54(2):185–196, 2016.

[19] P. C. Silva, C. Nicolet, P. Grillot, J.-L. Drommi, and B. Kawkabani. Assessment of power swings in hydropower plants through high-order modeling and eigenanalysis. *IEEE Transactions on Industry Applications*, 53(4):3345–3354, 2017.

[20] P. Gautam, J. Gummer, and J. Pott. Local penstock resonance resulting from turbine operation. In *Proc. of the IAHR Symposium (Montréal,)*, 2014.

[21] T. Jacob. Evaluation sur modèle réduit et prédiction de la stabilité de fonctionnement des turbines francis. page 226, 1993.